Available online at www.sciencedirect.com
ScienceDirect
Journal of Organometallic Chemistry 692 (2007) 2056–2063
Journal of Organometallic Chemistry
www.elsevier.com/locate/jorganchem

High-pressure NMR study of migratory CO-insertion in palladium–methyl complexes modified with C_s-symmetrical 1,4-diphosphines

Antonella Leone [a], Sebastian Gischig [b], Cornelis J. Elsevier [c], Giambattista Consiglio [a,*]

[a] *Eidgenössische Technische Hochschule, Institut für Chemie und Bioingenieurwissenschaften, Hönggerberg, Wolfgang-Pauli Strasse 10, CH-8093 Zürich, Switzerland*

[b] *Eidgenössische Technische Hochschule, Laboratorium für Anorganische Chemie, Hönggerberg, CH-8093 Zürich, Switzerland*

[c] *Molecular Inorganic Chemistry, J. H. Van 't Hoff Institute for Molecular Sciences (HIMS), Universiteit van Amsterdam, Nieuwe Achtergracht 166, 1018 WV Amsterdam, The Netherlands*

Received 4 November 2006; received in revised form 13 January 2007; accepted 16 January 2007
Available online 23 January 2007

Abstract

Carbonylation of the palladium complexes $[PdCH_3(P\hat{}P')Cl]$ (P^P′ = **1a**, **1b**, **1c**, **1d**, **1e**) and $[PdCH_3(P\hat{}P')(CH_3CN)](OTf)$ was investigated by means of high-pressure NMR with the determination of the half-life times $t_{1/2}$. The results were rationalized on the basis of the electronic properties of the diphosphines and the nature of the solvento ligand in the first coordination sphere. The crystal structures of the complexes $[Pd(\mathbf{1b})Cl_2]$ and $[Pd(\mathbf{1b})(H_2O)_2](OTf)_2$ are described (**1b** = 1-(diphenylphosphinomethyl)-2-[bis-(3- trifluoromethylphenyl)phosphinomethyl]benzene).

Keywords: High-pressure NMR; Carbonylation; Palladium complexes; Diphosphines; Half-life time

1. Introduction

High-pressure NMR has been successfully employed in studies mimicking the actual reactions conditions of many catalytic processes [1]. Applications include monitoring reactions under conditions similar to the catalytic reaction, stabilization and identification of the intermediates, measurements of kinetics and the study of exchange processes. Carbon monoxide migratory insertion into palladium–alkyl complexes modified with diphosphine ligands has been previously studied by means of HP-NMR spectroscopy. Geometric features of the ligands, such as flexibility and bite angle, influence the rate of carbon monoxide insertion in palladium–alkyl complexes [2]. Furthermore, the square planar intermediate *cis*-methyl(carbonyl)palladium diphosphine compound $[PdCH_3(CO)\{(S,S)\text{-BDPP}\}]BF_4$ ((*S*,*S*)-BDPP = (2*S*,4*S*)-2,4-bis(diphenylphosphino)pentane) was identified for the first time by means of a high-pressure NMR study [3]. High-pressure NMR techniques have also disclosed mechanistic details of the CO–propene co-polymerization catalyzed by palladium compounds containing the unsymmetrical bidentate phosphine-phosphite ligand (*R*,*S*)-BINAPHOS [4].

CO–ethene co-polymerization catalyzed by palladium complexes of dppe and dppp derivatives has recently been studied by HP-NMR to evaluate and rationalize the ligand control on the catalytic activity [5]. Palladium diacetate complexes with dppe, *rac*-2,3-dppp and *meso*-2,3-dppp ligands were tested in the ethene–CO co-polymerization. The activity of the catalyst precursors decreased in the order *meso*-2,3-dppb > *rac*-2,3-dppb > dppe [5].

C_s-symmetric 1,4-diphosphines **1b–d** (Fig. 1) have also been used as ligands in the co-polymerization of carbon

* Corresponding author. Tel.: +41 44 63 23552; fax: +41 44 63 21162.
E-mail address: consiglio@chem.ethz.ch (G. Consiglio).

0022-328X/$ - see front matter © 2007 Elsevier B.V. All rights reserved.
doi:10.1016/j.jorganchem.2007.01.020

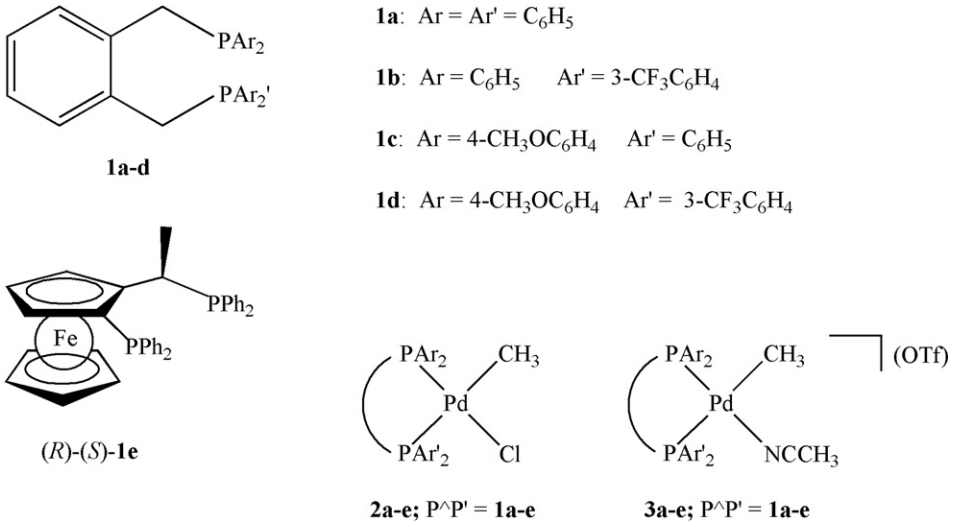

Fig. 1. Ligands **1a**–**e**, neutral complexes **2a**–**e**, cationic complexes **3a**–**e**.

monoxide and propene [6] and afforded highly regio- and stereoregular co-polymers. This was quite surprising, as the two non-symmetrical phosphorus moieties could have influenced the enantioface selection of the olefin.

In order to obtain a better understanding of this unexpected result, we have now investigated the carbonylation step of the complexes [$PdCH_3$(P^P′)Cl] (**2a**–**e**) and [$PdCH_3$(P^P′)(CH_3CN)](OTf) (**3a**–**e**) (Fig. 1) by kinetics. C_{2v}-symmetric compound **1a**, the parent compound of the series **1b**–**d**, can be taken as the reference for the study of the influence of electronic properties on the carbonylation rate. Compound **1e** ((*R*)-1-[(*S*)-2- (diphenylphosphine)ferrocenyl]ethyldiphenylphosphine) is a ferrocenyl diphosphine with a C_1-symmetry, in which the phosphorus atoms are electronically different due to the nature of the carbon backbone. It generates a six-membered palladadiphospha cycle in its Pd complexes, and is interesting for comparison. More specifically, we want to evaluate the influence of structural factors on the carbonylation rate and compare these to the complexes having a five-membered palladacycle.

The neutral and cationic complexes **2a**–**e** and **3a**–**e** (Fig. 1) were investigated in sapphire high-pressure NMR tubes by means of high pressure NMR techniques, with the aim to measure the carbonylation rate of these Pd complexes under conditions similar to those employed in the catalytic carbonylations.

2. Results

The neutral complexes [$PdCl(CH_3)$(P^P′)] (**2a**–**e**) (Fig. 1) were prepared by reaction of [PdCl (CH_3)(COD)] with the corresponding diphosphine ligand in CH_2Cl_2. With the exception of **2a** and **2e**, all complexes were obtained as mixtures of geometric isomers. All the complexes have been fully characterized prior to this study and their isomer distribution prior carbonylation had already been determined [7].

The rate of reaction of **1a**–**e** with CO was studied by using a high pressure NMR tube [8]. The samples of methylpalladium complexes with a concentration of 0.03 M in $CDCl_3$ were pressurized with 20 bar of CO at 20 °C and immediately inserted into the NMR probe for the measurement. The rates are reported as half-live times $t_{1/2}$ for the carbonylation reaction and were obtained following the decay of the phosphine signals due to the Pd–CH_3 complexes in the $^{31}P\{^1H\}$ NMR spectrum. The corresponding signals of the methyl groups in the ^1H NMR spectrum were not well resolved under the conditions of the experiment. The time at which the intensity was half of the initial value (measured before carbonylation) was taken as half-life time. Half-life values were determined and have been tabulated (Table 1) for each of the two isomers (the major, M, and the minor, m). Complex **2e**, containing the ferrocenyl diphosphine **1e**, was almost completely carbonylated at 20 °C when the first spectrum was acquired

Table 1
Reaction rates ($t_{1/2}$) for the carbonylation of **1a**–**e**[a]

Entry	M:m[b]	$t_{1/2}$, min[c]		M′:m′[d]
		M	m	
2a	1 isomer	58 ± 0.5		1 isomer
2b	5.2:1	34 ± 0.5	27 ± 0.5	3.1:1
2c	1.2:1	89 ± 0.5	96 ± 0.5	1.3:1
2d	6.3:1	82 ± 0.5	111 ± 0.5	7:1
2e	1 isomer[e]	<5 ± 0.5	<5 ± 0.5	2:1[f]

[a] Conditions: 0.03 M **2a**–**e** in $CDCl_3$, high-pressure NMR tube, 20 bar of CO, 296 K.
[b] Isomer ratio of the complexes **2a**–**e** before carbonylation (M = major isomer).
[c] $t_{1/2}$: time after which the amounts of starting compounds M and m were half.
[d] Ratio of acyl complexes, determined by high-pressure NMR experiments (M′: major isomer).
[e] CH_3 *trans* to PPh_2 directly bound to Cp.
[f] Major isomer, $C(O)CH_3$ *trans* to PPh_2 directly bound to Cp.

(i.e. within 2 min). Among the complexes modified with the C_s-symmetrical 1,4 diphosphine ligands, **2b** showed the smallest half-life time of the series; $t_{1/2}$ was 27 min for m and 34 min for M. Complex **2a**, obtained from the C_{2v}-symmetric ligand **1a**, showed a $t_{1/2}$ equal to 58 min. Longer half-life times were obtained for **2c** and **2d**, i.e. for the palladium complexes modified with the ligands **1c** and **1d**. For **2c** the values of $t_{1/2}$ for M and m were 89 and 96 min, respectively, while in the case of **2d** 82 min for M and 111 min for m were found. Apparently, the electron releasing 4-$CH_3OC_6H_4$ substituents at one P atom in **1c** and **1d** renders the carbonylation rate of their neutral palladium complexes slower when compared to the other cases. In all cases, the $t_{1/2}$ for the isomers M and m were rather similar. When the CO pressure was released, the complexes underwent partial decarbonylation upon standing. However, the acyl complexes are rather stable, as **4b** could be isolated in an independent experiment as a yellow solid.

The cationic complexes [Pd(CH_3)(P^P′)(CH_3CN)](OTf) (**3a**–**e**) were prepared in a mixture of CH_2Cl_2 and CH_3CN reacting one equivalent of the neutral complexes **2a**–**e** with 1.1 equivalent of silver triflate. As in the case of the neutral complexes, they exist as a mixture of two isomers, M, the major, and m, the minor.

As the CO migratory insertion in cationic complexes is known to proceed at very fast rate [2,9], the insertion reaction was monitored at low temperature. Samples of concentrations approximately 0.03 M were pressurized at −60 °C with 20 bar of CO and inserted in the probe precooled to −50 °C. The carbonylation was sometimes too fast to be monitored by NMR (Table 2). The half-life times $t_{1/2}$ were less than 5 min for the complexes **3c** and **3e**. While **3a** afforded a value of $t_{1/2}$ of 17 min, **3b** and **3d** showed a much slower carbonylation rate. The values are comparable with the $t_{1/2}$ of 62 min reported [5] for the migratory insertion in [Pd(CH_3)(*rac*-2,3-dppb)CO]$^+$. The isomer distribution observed after the carbonylation confirmed the results obtained from ambient pressure experiments. Apparently, the CO pressure does not influence the ratio M′:m′, where M′ and m′ are the major and the minor isomers of the acyl complexes, respectively.

Table 2
Reaction rates ($t_{1/2}$) for the carbonylation of **3a**–**e**[a]

Entry	M:m[b]	$t_{1/2}$, min[c]		M′:m′[d]
		M	m	
3a	1 isomer	17 ± 0.5		1 isomer
3b	1.8:1	96 ± 0.5	103 ± 0.5	2.6:1
3c	1.5:1	<5 ± 0.5	<5 ± 0.5	1.8:1
3d	2.5:1	74 ± 0.5	27 ± 0.5	3.2:1
3e	2:1[e]	<5 ± 0.5	<5 ± 0.5	2:1[f]

[a] Conditions: 0.03 M **3a**–**e** in $CDCl_3$, high-pressure NMR tube, 20 bar of CO, 223 K.
[b] Isomer ratio of the complexes **3a**–**e** before carbonylation (M = major isomer).
[c] $t_{1/2}$: time after which the amounts of starting compounds M and m were half.
[d] Ratio of acyl complexes, determined by high-pressure NMR experiments (M′: major isomer).
[e] Major isomer, CH_3 *trans* to PPh_2 directly bound to Cp.
[f] Major isomer, C(O)CH_3 *trans* to PPh_2 directly bound to Cp.

3. X-ray structures

Suitable single crystals for X-ray structure determinations were obtained by vapor diffusion of *n*-pentane into a $CHCl_3$ solution of the complexes at room temperature. ORTEP diagrams of **2b** ([$PdCl_2$(**1b**)]) and **3b** ([Pd(H_2O)$_2$(**1b**)](OTf)$_2$) with their atom numbering scheme are displayed in Figs. 2 and 3, respectively. Selected bond lengths and angles for **2b** are listed in Table 3. There are no intermolecular contacts that are significantly shorter than the sums of the van der Waals radii of the neighboring atoms. Complex **2b** crystallizes in the monoclinic space group *P*2(1)/*c* as brown–yellow platelets; it exhibits a slightly distorted square planar geometry as defined by the two phosphorus atoms and the two chlorides. The Cl(1) atom lies 0.1372 Å above the plane defined by P(1)–Pd(1)–P(2), while the Cl(2) atom is found 0.1198 Å below. The position of Cl(2) may reduce the orbital overlap with the metal, resulting in the longer bond distance measured for Pd(1)–Cl(2) compared to Pd(1)–Cl(1) of 2.3446(18) Å and 2.3501(17) Å, respectively. The Pd(1)–P distances (Pd(1)–P(1) = 2.2681 (18) Å and Pd(1)–P(2) = 2.2523(18) Å) fall in the range usually observed for palladium(II) diphosphine complexes. The longer Pd(1)–P(1) bond length reflects the more electron-withdrawing character of the P(3-$CF_3C_6H_4$)$_2$ moiety. The bite angle P(2)–Pd(1)–P(1) is 100.50(7)° and is similar to that measured for complexes containing similar ligands [7,10]. The deviation of the bite angle from the ideal value of 90° shows the geometric constraint induced by the seven-membered chelate ring and it similar to that of 103.08(3)° reported for the complex [PdCl(C(O)Et)(d′bpx)] containing the same type of ligand (*d*^{t}bpx = 1,2-bis(di-*tert*-butylphosphinomethyl)benzene) [11]. Other more flexible

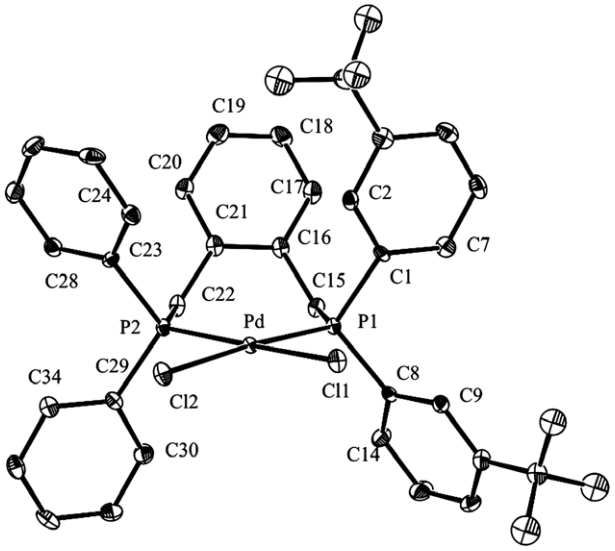

Fig. 2. ORTEP plot of [$PdCl_2$(**1b**)]. Thermal ellipsoids are set at the 30% probability level. Hydrogen atoms and disorder at CF_3 units are omitted for clarity.

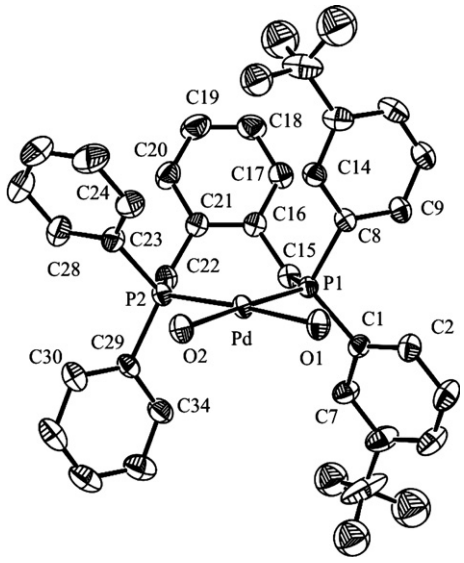

Fig. 3. ORTEP plot of $[Pd(\mathbf{1b})(H_2O)_2](OTf)_2$. Thermal ellipsoids are set at the 30% probability level. Hydrogen atoms, CF_3 disorder and counterions are omitted for clarity.

Table 3
Selected interatomic distances (Å) and angles (°) for $[Pd(\mathbf{1b})Cl_2]$

Bond length (Å)		Bond angle (°)	
Pd(1)–P(2)	2.2523(18)	P(2)–Pd(1)–P(1)	100.50(7)
Pd(1)–P(1)	2.2681(18)	P(2)–Pd(1)–Cl(1)	172.71(7)
Pd(1)–Cl(1)	2.3446(18)	P(1)–Pd(1)–Cl(1)	85.98(6)
Pd(1)–Cl(2)	2.3501(17)	P(2)–Pd(1)–Cl(2)	83.06(7)
		P(1)–Pd(1)–Cl(2)	175.40(7)
		Cl(1)–Pd(1)–Cl(2)	90.64(6)

1,4 diphosphines formed complexes with smaller bite angle, as that of approximately 92.9° found for [Pd(SCN)(NCS)(dppb)] [12].

The seven-membered chelate ring adopts a skew boat conformation with the benzylic carbons C(15) and C(22) almost coplanar. Both are below the plane defined by P(1)–Pd(1)–P(2) with a distance of 0.0674 Å for C(15) and of 0.0035 Å for C(22). The folding of the chelate ring is described by the angle of 110.9° between the least-squares planes defined by C(15), C(16), C(17), C(18), C(19), C(20), C(21), C(22) and C(15), C(22), Pd(1), P(1), P(2). The orientation of the benzene ring of the carbon backbone, which lies above the coordination ring, is further specified by the torsion angles P(1)–C(15)–C(16)–C(21) of −83.3(7)° and C(16)–C(21)–C(22)–P(2) of 88.7(7)°. Disorder involving two positions is observed at the bulky 3-CF_3 groups present at one phosphorus moiety. The two 3-$CF_3C_6H_4$ groups are tilted in such a way that the voluminous CF_3 substituents are not pointing to each other. One is directed toward the metal (*endo* position), the other is pointing away from the metal (*exo* position). Bond and torsion angles defining the orientation of the aryl groups in space are reported in Table 4.

Complex **3b** ($[Pd(H_2O)_2(\mathbf{1b})](OTf)_2$) crystallizes in the monoclinic space group $P2(1)/n$ as yellow platelets. The

Table 4
Bond and torsion angles (°) describing the orientation of the substituents for $[PdCl_2(\mathbf{1b})]$

Bond angle (°)	
C(8)–P(1)–C(1)	107.3(3)
C(29)–P(2)–C(23)	109.0(3)
Torsion angle (°)	
Pd(1)–P(1)–C(1)–C(2)	−34.0(6), 3-$CF_3C_6H_4$
Pd(1)–P(1)–C(8)–C(9)	−79.5(6), 3-$CF_3C_6H_4$
Pd(1)–P(2)–C(23)–C(24)	12.3(6), Ph
Pd(1)–P(2)–C(29)–C(34)	111.7(6), Ph

Table 5
Selected interatomic distances (Å) and angles (°) for $[Pd(\mathbf{1b})(H_2O)_2](OTf)_2$

Bond length (Å)		Bond angle (°)	
Pd(1)–O(1)	2.125(3)	O(1)–Pd(1)–O(2)	89.54(13)
Pd(1)–O(2)	2.135(3)	O(1)–Pd(1)–P(1)	85.75(10)
Pd(1)–P(1)	2.2239(11)	O(2)–Pd(1)–P(1)	175.27(10)
Pd(1)–P(2)	2.2248(11)	O(1)–Pd(1)–P(2)	174.78(11)
		O(2)–Pd(1)–P(2)	85.71(9)
		P(1)–Pd(1)–P(2)	98.99(4)

coordination sphere around the palladium is square planar with a slight distortion. A slight distortion is present in the first coordination sphere, where O(1) and O(2) are both below the P(1)–Pd(1)–P(2) plane with distances of −0.0816 Å and −0.0187 Å, respectively. The Pd–P bond lengths (Table 5) are comparable to those observed for the neutral and the cationic complexes of similar ligands [7,10], and are within the expected range for *cis*-chelated diphosphines at a palladium(II) center [13–17]. The observed Pd–OH_2 bond lengths are also within the normal range for related Pd–OH_2 complexes [14,15].

The bite angle of 98.99(4)° falls in the range expected for palladium complexes modified with *cis*-chelating diphosphine ligands and is, interestingly, smaller than that of the neutral complex $[Pd(\mathbf{1b})Cl_2]$. The seven-membered ring adopts a skew boat conformation as in the palladium dichloride complex. The benzylic carbons C(15) and C(22) are not perfectly coplanar with the plane defined by P(1)–Pd–P(2), but are lying 0.1810 Å and 0.0778 Å below it, respectively. The torsion angles C(16)–C(21)–C(22)–P(2) of 86.4(5)° and P(1)–C(15)–C(16)–C(21) of −83.0(5)° describe further the position of the two carbons. The atoms C(15), C(16), C(17), C(18), C(19), C(20), C(21), C(22) define a least-squares plane, which forms an angle of 112.4° with the plane containing C(15), C(22), P(1), Pd(1), P(2).

The position of the substituents at the phosphorus atoms is described through the bond and torsion angles reported in Table 6. For each phosphorus atom one substituent lies above and the other below the coordination plane, respectively.

4. Discussion

Carbonylation of the neutral complexes **2a**–**e** shows rate dependence both on structural and electronic factors. In a

Table 6
Bond and torsion angles (°) describing the orientation of the substituents for [Pd(**1b**)(H_2O)$_2$](OTf)$_2$

Bond angle (°)	
C(1)–P(1)–C(8)	109.9(2), 3-$CF_3C_6H_4$
C(23)–nP(2)–C(29)	110.0(2), Ph
Torsion angle (°)	
Pd(1)–P(2)–C(23)–C(28)	−173.0(4), Ph
Pd(1)–P(2)–C(29)–C(30)	112.9(4), Ph
Pd(1)–P(1)–C(1)–C(2)	−87.3(4), 3-$CF_3C_6H_4$
Pd(1)–P(1)–C(8)–C(9)	154.2(4), 3-$CF_3C_6H_4$

previous study [2] the carbonylation rate of a series of neutral palladium complexes [PdCl(CH_3)(PP)] was investigated, where PP = dppe, dppp, dppb, dppf. The carbonylation rate followed the order dppb ⩾ dppp ⩾ dppf ≫ dppe. It was suggested that a large bite angle, as well as the flexibility of the carbon backbone, facilitates the migratory insertion of CO. When the complexes investigated in this work are considered, it appears that **2e**, modified with a ferrocenyl diphosphine, reacted much faster than the complexes containing the 1,4 diphosphine ligands, no matter whether these are C_{2v}- or C_s-symmetric. The reactivity can be explained according to structural and electronic factors.

Structural data reported in the literature for the complex (dppb)Pd(NCS)(SCN) showed a bite angle of approximately 92.9° [12]. This value was close to the bite angles reported [18] for several Pd complexes modified with ferrocenyl diphosphine ligands, which ranged between 93° and 97°. The crystal structures of the complexes containing the C_s-symmetric ligands shown in Fig. 1 showed a bite angle of approximately 99–102° [7,10]. The 1,4-diphosphines, irrespective of the symmetry, are more flexible than 1,3-diphosphines and form a seven-membered ring once coordinated to the Pd. However, the carbonylation of the neutral complexes **2a**–**d** proceeds slower than in the case of the ferrocenyl diphosphine ligand, the $t_{1/2}$ of which is less than 5 min in the conditions of the experiment. In this case electronic factors may be responsible for the fast carbonylation rate, as one phosphorus moiety is directly connected to the cyclopentadienyl ring.

The differences in carbonylation rate found for the series **2a**–**d** should be completely ascribed to electronic factors, as the ligands **1a** and **1b**–**d** share the same carbon backbone. When the geometric isomerism was present, the species M and m displayed different reactivity toward carbon monoxide. For **2c** and **2d** the presence of the basic moiety P(4-$CH_3OC_6H_4$)$_2$ reduced apparently the carbonylation rate.

Whereas **1a** is a C_{2v}-symmetric ligand, the two bidentates in **1b**–**d** are non-equivalent. For the chloro complexes, carbonylation may take place through an associative mechanism, with the addition of CO to the metal center via a five-coordinate intermediate. Alternatively, and more likely, a dissociative pathway may take place, as it was proposed in the case of palladium and platinum containing phosphine ligands [2,19–23]. Migratory insertion of carbon monoxide would take place in the four-coordinated intermediate formed by substitution of a phosphine ligand with CO [23]. The dissociation of one P moiety could be the crucial step to explain the differences in rate observed in this study. In **1a** the dissociation of each of the two P atoms is equivalent from the energetic point of view, leading to the same intermediate. In the case of **1b**–**d** and **1e**, instead, the two P atoms are non-equivalent and the dissociation of a dentate from the Pd center may require different energy and lead to intermediates with different stability. These factors could account for the differences observed in the series **2a**–**d**.

The cationic complexes [Pd(CH_3)(P^P′)(CH_3CN)](OTf) (**3a**–**e**) underwent complete carbonylation much faster than their neutral counterparts; the $t_{1/2}$ was less than 5 min for **3c** and **3e** and equal to 17 min for **3a** at −50 °C. Slow carbonylation rate was observed for **3b** and **3d**. In this case the higher acidity of Pd, due to the 3-$CF_3C_6H_4$ groups at the P atoms, may cause CH_3CN to be strongly bonded to the metal and may explain their slower carbonylation rate. The coordination of this solvent molecule was indeed observed after the formation of the acyl complexes [7]. It is important to note that, depending on the ligand, there is a certain parallelism between the rates for the minor and the major isomers in both series of complexes. However, the parallelism does not subsist when the cationic and the neutral complexes are compared. At the moment we do not have any explanation in this respect.

The cationic complexes [Pd(CH_3)(P^P′)(CH_3CN)](OTf) are equivalent to the catalyst precursors employed in the co-polymerization of carbon monoxide and aliphatic olefins like propene [6]. The migratory insertion of CO in Pd–alkyl complexes modified with C_s-symmetric diphosphine ligands leads to a mixture of geometric isomers with different stability. Both are potentially able to insert the olefin and start a catalytic cycle. Thermodynamic and/or kinetic factors will control the progression of the chain and imply that only one intermediate is successful in transmitting the stereo- and the regiochemical information. Only in this way the high stereo- and regioregularity of the produced co-polymers can be explained.

5. Conclusions

The carbonylation of the neutral complexes **2a**–**e** and the cationic complexes **3a**–**e** was studied from a kinetic point of view. The determination of the half-live times $t_{1/2}$ for the neutral and cationic complexes **2a**–**e** and **3a**–**e** provided kinetic data for the carbonylation rate of neutral and cationic catalyst precursors. The carbonylation of cationic complexes was for some systems completed in less than 5 min at −50 °C, while the conversion of the neutral complexes to the corresponding acyl species could be easily followed at 20 °C.

For the Pd complexes containing C_s-symmetric diphosphine ligands, the existence of a geometric isomerism was proved also in presence of high pressures of CO. This suggests the existence of pairs of isomers also under the condi-

tions of the co-polymerization experiments, run out in presence of 80 bar of CO.

6. Experimental part

6.1. General remarks

Silver trifluoromethane sulfonate was purchased from Fluka. Benzene, CH_2Cl_2 and *n*-pentane used for the synthesis were of "puriss." grade, dried over molecular sieves and were purchased from Fluka. All the solvents used for recrystallyzation were of "puriss." quality and were used without further purification. The synthesis of the ligands **1b–d** has been already reported. **1a** was prepared with an analogous procedure. Ligand **1e** was kindly donated by S. Bronco. [PdCl(CH_3)(COD)] was prepared according to reported procedures [24,25]. The acyl complexes resulting from room pressure carbonylation experiments were analyzed on a Bruker Avance 500 spectrometer (frequency in MHz: ^{1}H: 500.13; ^{31}P: 202.45).

All HP-NMR experiments were performed on a Bruker DRX-300 MHz spectrometer with a 10 mm multinuclear broad-band probe: ^{1}H, 300.13 MHz; ^{31}P: 121.50 MHz employing 10 mm sapphire tubes [1]. Chemical shifts values are in parts per million relative to tetramethylsilane and H_3PO_4 as internal and external standards, respectively. $CDCl_3$ was purchased from Merck and was used without further purification.

The synthesis of the complexes **2b–d** and **3b–d** has been already described [7]. Compounds **2a**,**2e**, **3a** and **3e** were prepared in a similar manner.

6.2. Carbonylation of *2a, 2e, 3a* and *3e* at 1 bar CO pressure

Carbonylation of the complexes **2b–d** and **3b–d** at normal pressure was previously described [7].

6.3. Carbonylation of neutral complexes *2a* and *2e*

CO was bubbled (ca. 40 ml/min) through a metallic needle into a solution of 20–25 mg of the complex in 5 ml of $CDCl_3$ for ca. 40 min. The sample was then introduced into the probe and the first spectrum acquired after 5 min.

6.4. *[PdCl(C(O)CH$_3$)(1a)] (4a)*

^{31}P{^{1}H} NMR (202 MHz, $CDCl_3$, 25 °C): δ −2.2 (d, P_{trans} to C(O)CH_3; $^2J_{P-P} = 68.3$ Hz), 17.3 (d, P_{cis} to C(O)CH_3; $^2J_{P-P} = 68.3$ Hz).

6.5. *[PdCl(C(O)CH$_3$)(1e)] (4e)*

Two isomers in a 2:1 ratio result upon carbonylation (ratio determined from high-pressure NMR experiments). Major isomer, C(O)CH_3 *trans* to PPh_2; ^{31}P{^{1}H} NMR (202 MHz, $CDCl_3$, 25 °C): δ −2.3 (d, P_{trans} to C(O)CH_3; $^2J_{P-P} = 68.3$ Hz), 35.9 (P_{cis} to C(O)CH_3; $^2J_{P-P} = 68.3$ Hz). Minor isomer, C(O)CH_3 *trans* to CH(CH_3)PPh_2;^{31}P{^{1}H} NMR (202 MHz, $CDCl_3$, 25 °C): δ 11.8 (d, P_{trans} to C(O)CH_3; $^2J_{P-P} = 71.3$ Hz), 14.0 (P_{cis} to C(O)CH_3; $^2J_{P-P} = 71.3$ Hz).

6.6. Carbonylation of the cationic complexes *3a* and *3e*

A solution of 20–25 mg of the complex dissolved into 0.5 ml of $CDCl_3$ was cooled down to −60 °C. Carbon monoxide was bubbled for 5–10 min through a metallic needle into the NMR tube. The tube was then inserted in the pre-cooled NMR probe (−60 °C) and the first spectrum acquired after 5 min.

6.7. *[Pd(C(O)CH$_3$)(1a)(CH$_3$CN)](OTf) (5a)*

^{31}P{^{1}H} NMR (202 MHz, $CDCl_3$, −60 °C): δ 0.5 (br, P_{trans} to C(O)CH_3), 19.7 (br, P_{cis} to C(O)CH_3).

6.8. *[Pd(C(O)CH$_3$)(1e)(CH$_3$CN)](OTf) (5e)*

Two isomers in a ratio 2:1. Major isomer, C(O)CH_3 *trans* to PPh_2; ^{31}P{^{1}H} NMR (202 MHz, $CDCl_3$, −60 °C): δ 2.8 (d, P_{trans} to C(O)CH_3; $^2J_{P-P} = 62.4$ Hz), 42.1 (P_{cis} to C(O)CH_3; $J_{P-P} = 62.4$ Hz). Minor isomer, C(O)CH_3 *trans* to CH(CH_3)PPh_2; ^{31}P{^{1}H} NMR (202 MHz, $CDCl_3$, −60 °C): δ 16.0 (d, P_{trans} to C(O)CH_3; $^2J_{P-P} = 71.3$ Hz), 24.9 (P_{cis} to C(O)CH_3; $J_{P-P} = 71.3$ Hz).

6.9. High-pressure carbonylation of the neutral complexes *[PdCl(CH$_3$)(P^P′)] (2a–e)*

0.03 M solutions of the complexes **2a–e** in $CDCl_3$ were transferred into a sapphire tube and pressurized with carbon monoxide to a pressure of 20 bar. The tube was shaken three times and transferred directly into the NMR spectrometer. The first spectrum was acquired after 5 min.

6.10. High-pressure carbonylation of cationic complexes *[Pd(CH$_3$)(P^P′)(CH$_3$CN)](OTf) (3a–e)*

0.03 M solutions of the complexes **3a–e** in $CDCl_3$ were transferred in a sapphire tube and cooled down to −60 °C. The sapphire tube was then pressurized with 20 bar of carbon monoxide at this temperature. The tube was shaken three times and transferred directly into the spectrometer, which had been pre-cooled to −50 °C. The first spectrum was obtained after 5 min.

7. X-ray crystallography

X-ray structures were measured on a Bruker CCD diffractometer (Bruker SMART PLATFORM, with CCD detector, graphite monochromated, Mo Kα radiation). The program SMART served for the data collection. Integration was performed with SAINT. The structure solution and refinement on F^2 were accomplished with SHELXTL 97. Model plots

Table 7
Crystal data, measurement and refinement parameters for [$PdCl_2$(**1b**)] and [Pd(**1b**)(H_2O)$_2$](OTf)$_2$

Identification code	[$PdCl_2$(**1b**)]	[Pd(**1b**)(H_2O)$_2$](OTf)$_2$
Empirical formula	$C_{34}H_{26}Cl_2F_6P_2Pd$	$C_{36}H_{30}F_{12}O_8P_2PdS_2$
Formula weight	787.79	1051.06
Temperature (K)	150(2)	298(2)
Wavelength (Å)	0.71073	0.71073
Crystal system	Monoclinic	Monoclinic
Space group	*P*2(1)/*c*	*P*2(1)/*n*
Unit cell dimensions		
a (Å)	13.0001(16)	10.1721(15)
b (Å)	7.7646(9)	24.846(4)
c (Å)	31.960(4)	17.393(3)
α (°)	90	90
β (°)	93.419(3)	96.264(3)
γ (°)	90	90
Volume (Å^3)	3220.3(7)	4369.6(11)
Z	4	4
D_{calc} (mg cm^{-3})	1.625	1.598
Absorption coefficient (mm^{-1})	0.901	0.692
F(000)	1576	2104
Crystal size (mm)	0.15 × 0.14 × 0.13	0.41 × 0.22 × 0.09
Theta range for data collection (°)	1.96–26.38	2.17–26.37
Limiting indices	$-16 \leqslant h \leqslant 16$, $-8 \leqslant k \leqslant 9$, $-25 \leqslant l \leqslant 39$	$-12 \leqslant h <= 12$, $-31 \leqslant k \leqslant 30$, $-21 \leqslant l <= 21$
Reflections collected	19984	38726
Independent reflections	6578 ($R_{int} = 0.0450$)	8902 ($R_{int} = 0.0287$)
Completeness to theta	=26.38° 99.8%	=26.37° 99.7%
Refinement method	Full-matrix least-squares on F^2	Full-matrix least-squares on F^2
Data/restrains/parameters	6578/24/406	8902/33/563
Goodness-of-fit on F^2	1.215	1.042
Final *R* indices [$I > 2$sigma(I)]	$R_1 = 0.0779$, $wR_2 = 0.1668$	$R_1 = 0.0597$, $wR_2 = 0.1628$
R indices (all data)	$R_1 = 0.0940$, $wR_2 = 0.1733$	$R_1 = 0.0724$, $wR_2 = 0.1741$
Largest difference peak and hole (e Å^{-3})	1.734 and −1.095	1.058 and −0.759

were made with ORTEP32. All non-hydrogen atoms were refined freely with anisotropic displacements. The hydrogen atoms were refined at calculated positions riding on their carrier atoms. Weights are optimized in the final refinement cycles. Table 7 shows the crystallographic data for the compounds [Pd(**1b**)Cl_2] and [Pd(**1b**)(H_2O)$_2$](OTf)$_2$.

Acknowledgments

HP-NMR experiments were carried out at the Van't Hoff Institute for Molecular Sciences of the University of Amsterdam (Amsterdam, The Netherlands). The authors thank J.M. Ernsting for the technical support. COST action D17 is acknowledged for the STSM of A.L. at the University of Amsterdam, The Netherlands.

Appendix A. Supplementary data

CCDC 281606 and 281607 contain the supplementary crystallographic data for [Pd(**1b**)Cl_2] and [Pd(**1b**)(H_2O)$_2$]-(OTf)$_2$. These data can be obtained free of charge via http://www.ccdc.cam.ac.uk/conts/retrieving.html, or from the Cambridge Crystallographic Data Centre, 12 Union Road, Cambridge CB2 1EZ, UK; fax: (+44) 1223-336-033; or e-mail: deposit@ccdc.cam.ac.uk. Supplementary data associated with this article can be found, in the online version, at doi:10.1016/j.jorganchem.2007.01.020.

References

[1] I.T. Horvath, J.M. Millar, Chem. Rev. 91 (1991) 1339, and references cited therein;
C.J. Elsevier, J. Mol. Catal. 92 (1994) 285;
I.T. Horvath, G. Kiss, R.A. Cook, J.E. Bond, P.A. Stevens, J. Rabai, E.J. Mozeleski, J. Am. Chem. Soc. 120 (1998) 3133.
[2] G.P.C.M. Dekker, C.J. Elsevier, K. Vrieze, P.W.N.M. van Leeuwen, Organometallics 11 (1992) 1598.
[3] I. Toth, C.J. Elsevier, J. Am. Chem. Soc. 115 (1993) 10388.
[4] K. Nozaki, T. Hiyama, S. Kacker, I.T. Horvath, Organometallics 19 (2000) 2031.
[5] C. Bianchini, H.M. Lee, A. Meli, W. Oberhauser, M. Peruzzini, F. Vizza, Organometallics 21 (2002) 16.
[6] A. Leone, G. Consiglio, Helv. Chim. Acta 88 (2005) 210.
[7] A. Leone, S. Gischig, G. Consiglio, J. Organomet. Chem. 691 (2006) 4816.
[8] D.C. Roe, J. Magn. Reson. 63 (1985) 388.
[9] C.S. Shultz, J. Ledford, J.M. DeSimone, M. Brookhart, J. Am. Chem. Soc. 122 (2000) 6351.
[10] A. Leone, S. Gischig, G. Consiglio, J. Mol. Catal. (in press).
[11] W. Clegg, G.R. Eastham, M.R.J. Elsegood, B.T. Heaton, J.A. Iggo, R.P. Tooze, R. Whyman, S. Zacchini, Organometallics 21 (2002) 1832.
[12] A.J. Paviglianiti, D.J. Minn, W.C. Fultz, J.L. Burmeister, Inorg. Chim. Acta 159 (1989) 65.

[13] F. Ozawa, A. Kubo, Y. Matsumoto, T. Hayashi, E. Nishioka K. Yanagi, K. Moriguchi, Organometallics 12 (1993) 4188.
[14] P.J. Stang, D.H. Cao, G.T. Poulter, A.M. Arif, Organometallics 14 (1995) 1110.
[15] F. Benetollo, R. Bertani, G. Bombieri, L. Toniolo, Inorg. Chim. Acta 233 (1995) 5.
[16] T. Hayashi, M. Konishi, Y. Kobori, M. Kumada, T. Higuchi K. Hirotsu, J. Am. Chem. Soc. 106 (1984) 158.
[17] W.L. Steffen, G.J. Palenik, Inorg. Chem. 15 (1976) 2432.
[18] C. Gambs, G. Consiglio, A. Togni, Helv. Chim. Acta 84 (2001) 3105.
[19] P.E. Garrou, R.F. Heck, J. Am. Chem. Soc. 98 (1976) 4115.
[20] G.K. Anderson, R.J. Cross, Acc. Chem. Res. 17 (1984) 67.
[21] P.W.N.M. Van Leeuwen, C.F. Roobeek, J.H.G. Frijns, A.G. Orpen, Organometallics 9 (1990) 1211.
[22] G.P.C.M. Dekker, A. Buijs, C.J. Elsevier, K. Vrieze, P.W.N.M. van Leeuwen, W.J.J. Smeets, A.L. Spek, Y.F. Wang, C.H. Stam, Organometallics 11 (1992) 1937.
[23] R. van Asselt, E. Gielens, R.E. Rulke, K. Vrieze, C.J. Elsevier, J. Am. Chem. Soc. 116 (1994) 977.
[24] R.E. Rulke, I.M. Han, C.J. Elsevier, K. Vrieze, P. van Leeuwen, C.F. Roobeek, M.C. Zoutberg, Y.F. Wang, C.H. Stam, Inorg. Chim. Acta 169 (1990) 5.
[25] R.E. Rulke, J.M. Ernsting, A.L. Spek, C.J. Elsevier, P. van Leeuwen, K. Vrieze, Inorg. Chem. 32 (1993) 5769.